

Elastic and inelastic scattering of electrons by atomic hydrogen at intermediate energies in a coupled-channel second-order potential model

B H Bransden^{†¶}, T Scott[‡], R Shingal[§] and R K Roychoudhury^{||}

[†] Joint Institute for Laboratory Astrophysics, University of Colorado, and National Bureau of Standards, Boulder, Colorado 80309, USA

[‡] AEE, Winfrith, Dorset, England

[§] University of Durham, Durham DH1 3LE, England

^{||} The Indian Statistical Institute, Calcutta, India

Received 16 August 1982

Abstract. A second-order model employing a pseudostate expansion in intermediate states is applied in a 1s–2s–2p coupled-channel formalism to electron scattering by atomic hydrogen in the energy range 54 to 200 eV. Although the model predicts cross sections for elastic scattering, and excitation of the $n = 2$ levels, which are in reasonable accord with the experimental data, the predicted results for the angular correlation parameters show little improvement over the 1s–2s–2p close-coupling model.

1. Introduction

In a previous paper (Scott and Bransden 1981, afterwards referred to as I), the second-order optical potential method of Bransden and Coleman (1972) was applied to the elastic scattering of electrons by atomic hydrogen in a one-channel model. The closure approximation was avoided by expanding the intermediate states occurring in second-order matrix elements on a finite basis of pseudostates, and the results obtained were very close to those of McCarthy *et al* (1982), who summed over the intermediate states numerically, using the exact hydrogenic discrete and continuum orbitals. In this paper, the same model is applied to a multichannel system coupling the 1s, 2s and 2p levels of atomic hydrogen, allowing the calculation of the cross sections for excitation of the 2s, 2p₀ and 2p_{±1} level, as well as for elastic scattering. Cross sections in the 1s+2s+2p coupled-channel system with second-order potentials have been calculated previously by Bransden and Noble (1976a, b), who made two approximations which have been avoided in the present work. These were: (i) the sum over intermediate states was carried out by closure, (ii) the coupled equations were solved in a straight-line impact parameter approximation. Previously Winters *et al* (1974) showed that while the impact parameter method is accurate for large values of the angular momentum of the scattered electron, it fails in the energy region under consideration (50 to 200 eV) for $l \leq 8$. Correspondingly, although total cross sections are determined accurately in the impact parameter approximation, differential cross

[¶] Permanent address: The University of Durham, Durham DH1 3LE, England.

sections are inaccurate except at small angles ($\theta \leq 20^\circ$) even at comparatively high energies (Reid *et al* 1977). It is true that the semiclassical approximation can be used, down to much lower energies (~ 20 eV) and to larger angles, by integrating the coupled equations along a non-linear trajectory (Bransden and Noble 1976c, Martir *et al* 1982). However, in this work we follow the procedure of I and use a full partial-wave treatment to calculate elastic scattering and $n = 2$ excitation cross sections in the energy range 54 to 200 eV.

2. Formulation and computational details

The general formalism of the second-order-potential model has been sufficiently described in paper I (also see Bransden and Coleman 1972, Bransden and McDowell 1977, Bransden 1982). In the notation of I, the basic coupled equations to be solved are:

$$(\nabla^2 + k_n^2)F_n(\mathbf{x}) = \sum_{m=0}^M \left(V_{nm}(\mathbf{x})F_m(\mathbf{x}) + \int d\mathbf{r} (W_{nm}^s(\mathbf{x}, \mathbf{r}) + K_{nm}(\mathbf{x}, \mathbf{r}))F_m(\mathbf{r}) \right) \\ n = 0, 1, 2, \dots, M. \quad (1)$$

There are two sets of equations, one for each spin state S , and the indices n and m run over the $1s$, $2s$, $2p_0$ and $2p_{\pm}$ channels of the electron-hydrogen-atom system. The potential matrices V_{nm} and W_{nm}^s are the usual direct and exchange potentials arising in the close-coupling equations while K_{nm} is the direct part of the second-order-potential matrix:

$$K_{nm}(\mathbf{x}, \mathbf{r}) = \sum_{q>M} V_{nq}(\mathbf{x})G_0(k_q^2; \mathbf{x}, \mathbf{r})V_{qm}(\mathbf{r}). \quad (2)$$

The sum over q runs over all intermediate states and pseudostates except the $1s$, $2s$, $2p_0$ and $2p_{\pm 1}$ states and G_0 is the appropriate free-particle Green's function.

Although, as emphasised by Walters (1980) and Ermolaev and Walters (1979), second-order exchange may be often of importance, the close agreement at 50 eV, and above, between the results of I and those of McCarthy *et al* (1981, 1982), who included the second-order exchange potential in their model of elastic scattering, suggests that at energies above 50 eV, this effect is of minor importance. For this reason, second-order exchange has not been included in the present calculation. In the case of elastic scattering, Byron and Joachain (1981) have shown convincingly that the third-order contribution to the direct part of the optical potential has little effect on the differential cross section, the maximum contribution from this term being of the order of ten per cent at small angles. It is, of course, possible that the third-order terms are more significant for excitation, but we feel that this is unlikely and we have not allowed for these terms in our calculation. It should be noted that as far as elastic scattering is concerned that part of the third-order contribution due to $2s$ - $2p$ coupling is automatically taken into account by the model.

To obtain numerical solutions of the coupled equations (1), a standard partial-wave decomposition was made to obtain sets of coupled radial equations. These radial equations were solved along the lines described in I, treating the non-local kernels iteratively. To avoid excessive expenditure of computer time, we followed the procedure of Kingston *et al* (1976), who omitted the exchange kernels for values of the total angular momentum L for which it could be shown that the singlet and triplet

cross sections were equal to within sufficient accuracy, and who employed the unitarised Born approximation to estimate the scattering amplitudes for large L . In our calculations, the exchange kernels could be omitted for $L > 10$ at 54 and 100 eV; and $L > 8$ at 200 eV. For $L \geq 20$ the amplitudes were calculated from the unitarised Born approximation. We followed Kingston *et al* in ensuring that the partial-wave amplitudes in the regions $L \leq 20$ and $L > 20$ joined smoothly, to avoid spurious oscillations in the differential cross section at large angles.

The full pseudostate basis, employed for the intermediate states q in (2), was defined in paper I. To economise on computer time and storage, a slightly smaller basis was used in the present calculations in which the d and f states were omitted. In the one-channel model, this restriction of the basis is known not to be serious. Thus, the basis contained four $l = 0$ states, and three with $l = 1$. All these pseudostates are orthogonal to the 1s, 2s and 2p hydrogenic states which are allowed for explicitly in the coupled equations.

3. Numerical results

3.1. Elastic scattering

Our calculated cross sections[†] at 54, 100 and 200 eV for elastic scattering, and total cross sections calculated from the optical theorem are shown in table 1, together with the experimental data and cross sections from some other related models. Let us first consider the situation at 54 eV. The present results are close to those of the one-channel model of I (column B), over an angular range $40 < \theta < 100^\circ$; but are significantly smaller in the forward and backward directions, and in less good agreement with the experiment. A comparison with the results of an R -matrix calculation (see column E) by Fon *et al* (1981) shows close agreement except at very large angles where the R -matrix cross section is somewhat larger. The pseudostate basis employed in the R -matrix calculations was rather small, consisting of $\bar{3}s$, $\bar{3}p$ and $\bar{3}d$ levels (apart from the 1s, 2s and 2p real states). It is possible that the larger cross sections obtained in the model of I and by McCarthy *et al* (1982) would be regained if the d and f pseudostates were included and the larger cross sections obtained at large angles in the R -matrix model may be due to the inclusion of the $\bar{3}d$ pseudostate. Very similar cross sections have been obtained by Callaway *et al* (1975), who also employed a pseudostate expansion, like that used in I; however, the full expansion was only employed in the calculation of partial waves with $L \leq 3$, higher partial waves being treated more approximately. In contrast, the cross sections computed by Byron and Joachain (1981) (column C), using a single-channel local optical potential, are very close to the present results for $\theta > 35^\circ$, but rise above our results and above the data at small angles. The connection between the results of the EBS model (Byron and Joachain 1977) and the optical model results has been discussed by Byron and Joachain (1981). As we have mentioned above, the explicit second-order optical potential model of McCarthy *et al* (1982), in which the sum over all important intermediate states is effected numerically, produces cross sections in a one-channel implementation very close to those of I. Finally, a comparison can be made with the results of Bransden and Noble (1976b, c), who used the same basic model as in the present work, but who used closure to sum over intermediate states and also an impact parameter

[†] Differential cross sections at 5° intervals are available on request.

Table 1. Differential and total cross sections for the elastic scattering of e^- by $H(1s)$ (cross sections in units of a_0^2).

$\theta(\text{deg})$	54 eV					100 eV					200 eV				
	Expt	A	B ^a	C ^a	D ^a	E ^a	Expt	A	B	C	D	Expt	A	C	D
0	—	7.4	10.2	13.0	—	8.6	—	4.9	4.9	8.5	—	—	2.9	5.7	—
10	5.0(5)	3.8	5.0	6.3	4.2	3.8	—	1.91	1.9	2.6	—	—	0.98	1.14	—
20	2.2(2)	1.7	2.2	2.6	2.0	1.69	1.1(1)	0.80	0.80	0.90	0.89	0.42(4)	0.38	0.39	0.44
30	1.1(1)	0.89	1.1	1.14	1.06	0.87	0.51(5)	0.38	0.37	0.38	0.44	0.17(2)	0.15	0.15	0.17
40	0.55(6)	0.50	0.54	0.54	0.59	0.49	0.29(3)	0.19	0.18	0.18	0.21	0.071(7)	0.062	0.062	0.073
60	0.21(2)	0.18	0.18	0.166	0.20	0.20	0.072(7)	0.059	0.054	0.054	0.061	0.019(2)	0.017	0.016	0.018
80	0.099(12)	0.078	0.080	0.068	0.091	0.096	0.030(3)	0.024	0.023	0.023	0.026	0.0086(9)	0.0065	0.0063	0.0071
100	0.056(7)	0.041-	0.045	0.038	0.050	0.055	0.016(1)	0.013	0.013	0.012	0.013	0.0041(4)	0.0033	0.0032	0.0035
120	0.035(3)	0.025	0.030	0.026	0.032	0.037	0.0092(9)	0.0082	0.0082	0.0082	0.0083	0.0027(4)	0.0020	0.0020	0.0022
140	0.027(3)	0.018	0.023	0.020	0.024	0.028	0.0065(7)	0.0060	0.0060	0.0060	0.0055	0.0018(3)	0.0014	0.0014	0.0016
160	—	0.015	—	0.017	—	0.024	—	0.0050	—	0.0046	—	—	0.0012	0.0012	—
180	—	0.015	—	0.016	—	0.023	—	0.0048	—	0.0043	—	—	0.0012	0.0011	—
σ_{el}	3.83	3.18	3.83	4.16	4.30	3.30	1.75	1.45	1.45	1.54	1.50	0.669	0.58	0.631	0.672
σ_{tot}	10.40	14.1	11.9	13.5	10.41	—	7.28	8.03	7.31	7.68	6.78	4.44	3.70	4.38	3.94

Expt, differential cross section (Williams 1975); total cross sections (de Heer *et al* 1977), only two significant figures are tabulated with the error given in brackets.
A, present results; B, one-channel model (Scott and Bransden 1981); C, local optical model (Byron and Joachain 1981); D, explicit optical model (McCarthy *et al* 1982); E, R-matrix model (Fon *et al* 1981).
^a 50 eV.

approximation. Their results, which are not shown in the table, are about 20% greater than the present ones in the forward direction and diminish a little more rapidly with increasing scattering angle.

At 100 eV and above, the one-channel differential cross sections of I are virtually identical with those of the three-channel model. These cross sections are also very close to those of the one-channel closure model of Winter *et al* (1974), and as far as elastic scattering is concerned, these three models should be identical at all higher energies. In addition, at both 100 and 200 eV, with the exception of the very-small-angle region $\theta \leq 10^\circ$, the results of the local third-order optical model of Byron and Joachain are very close to those of the three-channel model, and only differ in detail from those of the explicit optical model of McCarthy *et al* (1982). Byron and Joachain (1981) have published cross sections at energies up to 500 eV and except in the forward direction it can be assumed that the present model would provide the same elastic scattering cross sections. At both 100 and 200 eV, the general agreement with the experimental data is good, although at certain angles there are discrepancies of up to 25%, which are difficult to attribute to the failure of the theoretical models. At 100 and 200 eV, the cross sections of the impact parameter three-channel model become closer to those of the present work; but the agreement is still not very close.

3.2. Excitation of the $n = 2$ levels

Our calculated differential cross sections for excitation of the 2s level of hydrogen are shown in table 2, and of the 2p level in table 3. The calculated values for the differential cross section for the excitation of the $n = 2$ levels are shown in figures 1(a), (b) for 100 and 200 eV, respectively, together with the experimental data of Williams and Willis (1975). Also shown in tables 2 and 3 are the results of a three-state (1s–2s–2p) close-coupling calculation of Kingston *et al* (1976). As in the present model, Kingston *et al* employed the unitarised Born approximation to calculate the higher partial-wave amplitudes. We have verified that our results agree satisfactorily with theirs, when the second-order-potential terms are dropped. Neither the three-state close-coupling nor the present results agree with the large-angle data of Williams and Willis at 100 eV, but agreement between the present results and experiment is good at 200 eV. In the case of the 2p cross section, the most significant difference at 100 and 200 eV between the second-order-potential model and the three-state close-coupling model, is that the second-order potential lowers the cross section in an angular region in the vicinity of $20^\circ \leq \theta \leq 40^\circ$. At 54 eV, this lowering of the cross section is also seen, but the cross section in the second-order potential model is also smaller than that of the close-coupling model in the backward direction $\theta > 100^\circ$. In the case of the 2s cross section the difference between the second-order-potential and close-coupling models is much greater, particularly in the forward direction in which the second-order-potential cross sections are much smaller. As pointed out by Byron and Latour (1976), this is not unexpected because the contributions to the amplitudes which are neglected in the close-coupling approximation are known to be peaked near the forward direction. At 54 eV, the results of Callaway *et al* (1975) using a pseudostate basis are available for comparison and these are also shown in tables 2 and 3. These results are different in detail from either of the other models, but too much should not be made of this, since only the partial waves with $L \leq 3$ were computed from the full pseudostate model, those for $L > 3$ being calculated approximately. In particular the 2p cross section of the Callaway *et al* model shows a deep minimum

Table 2. Differential and total cross sections for excitation of the 2s level of hydrogen by electron impact (cross sections in a_0^2)[†].

$\theta(\text{deg})$	Expt	54 eV				100 eV				200 eV			
		A	A'	B	C	A	A'	C	A	A'	C		
0	—	8.3^{-1}	1.41	2.93	3.3	9.3^{-1}	1.3	3.57	1.20	1.21	3.33		
10	$3.8^{-1}(13)$	1.6^{-1}	2.8^{-1}	$5.9^{-1\frac{1}{2}}$	5.8^{-1}	3.0^{-1}	3.0^{-1}	3.65^{-1}	2.5^{-1}	2.5^{-1}	2.6^{-1}		
20	$9.0^{-2}(18)$	8.5^{-2}	6.7^{-2}	$9.9^{-2\frac{1}{8}}$	1.23^{-1}	6.8^{-2}	6.6^{-2}	8.8^{-2}	2.3^{-2}	2.1^{-2}	2.8^{-2}		
30	$3.5^{-2}(4)$	2.5^{-2}	1.7^{-2}	2.1^{-2}	4.4^{-2}	1.10^{-2}	1.03^{-2}	2.0^{-2}	2.8^{-3}	2.6^{-3}	4.2^{-3}		
40	$1.65^{-2}(128)$	6.5^{-3}	—	—	1.90^{-2}	3.4^{-3}	—	7.6^{-3}	1.16^{-3}	—	1.56^{-3}		
60	$1.01^{-2}(48)$	4.2^{-3}	—	6.3^{-3}	9.9^{-3}	1.6^{-3}	—	2.7^{-3}	2.9^{-4}	—	4.1^{-4}		
80	$6.2^{-3}(25)$	3.1^{-3}	—	—	6.7^{-3}	7.6^{-4}	—	1.28^{-3}	1.35^{-4}	—	1.61^{-4}		
100	$3.9^{-3}(11)$	2.1^{-3}	—	—	4.4^{-3}	4.2^{-4}	—	7.1^{-4}	5.6^{-5}	—	8.0^{-5}		
120	$2.8^{-2}(10)$	1.7^{-3}	—	2.5^{-3}	3.3^{-3}	2.8^{-4}	—	4.7^{-4}	4.1^{-5}	—	5.1^{-5}		
140	$2.2^{-3}(9)$	1.5^{-3}	—	—	2.8^{-3}	2.2^{-4}	—	3.6^{-4}	2.7^{-5}	—	3.8^{-5}		
160	—	1.4^{-3}	—	—	2.5^{-3}	1.90^{-4}	—	3.1^{-4}	2.5^{-5}	—	3.3^{-5}		
180	—	1.4^{-3}	—	8.2^{-4}	2.4^{-3}	1.64^{-4}	—	3.0^{-4}	4.1^{-5}	—	3.2^{-5}		
σ_{2s}	0.166	0.124	0.13	0.229	0.317	0.110	0.113	0.182	0.075	0.075	0.094		
						$(\sigma_{2s}(\text{expt}) = 0.14)$			$(\sigma_{2s}(\text{expt}) = 0.10)$				

Expt, differential cross sections, Williams (1981); total cross section, Kaupilla *et al* (1970), corrected for cascading, only two significant figures are tabulated with the error in brackets.

A, Present results; A', impact parameter model (Bransden and Noble 1976a, b); B, pseudostate coupled-channel model (Callaway *et al* 1975); C, three-state close-coupling model (Kingston *et al* 1976).

[†] The superscripts in the table indicate the power of ten by which the entry should be multiplied.

[‡] 9°.

[§] 18°.

Table 3. Differential and total cross sections for excitation of the 2p level of hydrogen by electron impact (cross sections in a_0^2)†.

$\theta(\text{deg})$	Expt	54 eV				100 eV				200 eV			
		A	A'	B	C	A	A'	C	A	A'	C	A	C
0	—	41.2	37.3	13.7	39.0	97.3	91.2	88.6	251	209	201	—	—
10	7.5 (7)	7.4	7.2	9.3‡	7.8	4.2	4.4	4.6	1.46	1.54	1.57	—	—
20	1.04 (11)	7.9 ⁻¹	1.00	1.34§	1.18	2.1 ⁻¹	3.1 ⁻¹	3.2 ⁻¹	2.4 ⁻²	4.2 ⁻²	3.8 ⁻²	—	—
30	1.57 ⁻¹ (21)	7.8 ⁻²	1.8 ⁻¹	1.26 ⁻¹	1.99 ⁻¹	1.20 ⁻²	3.3 ⁻²	3.0 ⁻²	1.6 ⁻³	3.2 ⁻³	2.4 ⁻³	—	—
40	4.4 ⁻² (7)	1.4 ⁻²	—	—	4.7 ⁻²	3.0 ⁻³	—	6.4 ⁻³	5.2 ⁻⁴	—	6.7 ⁻⁴	—	—
60	1.19 ⁻² (21)	6.1 ⁻³	—	8.8 ⁻³	1.11 ⁻²	1.35 ⁻³	—	1.54 ⁻³	2.0 ⁻⁴	—	1.9 ⁻⁴	—	—
80	4.1 ⁻³ (9)	3.5 ⁻³	—	—	4.7 ⁻³	6.3 ⁻⁴	—	7.4 ⁻⁴	1.08 ⁻⁴	—	9.5 ⁻⁵	—	—
100	2.2 ⁻³ (5)	2.0 ⁻³	—	—	2.6 ⁻³	3.9 ⁻⁴	—	4.7 ⁻⁴	6.6 ⁻⁵	—	6.4 ⁻⁵	—	—
120	1.59 ⁻³ (36)	1.36 ⁻³	—	6.1 ⁻⁴	1.69 ⁻³	2.8 ⁻⁴	—	3.5 ⁻⁴	6.0 ⁻⁵	—	4.8 ⁻⁵	—	—
140	1.03 ⁻³ (28)	8.4 ⁻⁴	—	—	1.31 ⁻³	2.5 ⁻⁴	—	2.8 ⁻⁴	4.7 ⁻⁵	—	4.1 ⁻⁵	—	—
160	—	6.4 ⁻⁴	—	—	1.12 ⁻³	2.1 ⁻⁴	—	2.4 ⁻⁴	5.1 ⁻⁵	—	3.7 ⁻⁵	—	—
180	—	5.8 ⁻⁴	—	6.5 ⁻³	1.09 ⁻³	2.3 ⁻⁴	—	2.3 ⁻⁴	3.1 ⁻⁵	—	3.3 ⁻⁵	—	—
σ_{2p}	2.79 (24) ^a	2.56	2.63	2.69	2.85	2.11	2.07	2.13	1.59	1.51	1.42	—	—
						($\sigma_{2p}(\text{expt}) = 2.3$) ^b			$\sigma_{2p}(\text{expt}) = 1.7$) ^b				

Expt, differential cross section.

^a σ_{2p} , Williams (1981).^b σ_{2p} interpolated from the data of Long *et al* (1968) renormalised by Bransden and McDowell (1978).A, Present results; A', impact model (Bransden and Noble 1976a, b); B, pseudostate coupled-channel model (Callaway *et al* 1975); C, three-state close-coupling model (Kingston *et al* 1976).

† The superscripts in the table indicate the power of ten by which the entry should be multiplied.

‡ 9°.

§ 18°.

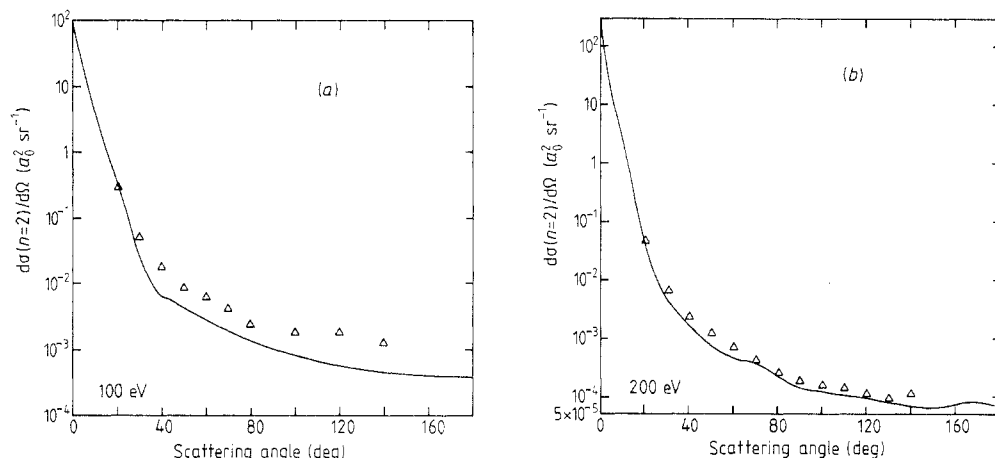


Figure 1. The differential cross section for excitation of the $n = 2$ levels of hydrogen (a) at 100 eV and (b) at 200 eV. Δ , Experimental data (Williams and Willis 1975); —, present values.

near 120° , not shown in the other models, which is difficult to understand. It is also interesting to compare the present results with those of Bransden and Noble (1976a, b) in the impact parameter closure model. By 200 eV the agreement for the 2s cross section is very good at small angles $\theta \leq 20^\circ$ (for which the impact parameter treatment should be accurate). However, for the 2p cross section the differences even at 200 eV are larger than one would have expected, and this may be a sign that the pseudostate basis set is not sufficiently large, or that the average energy used in the closure approximation was not optimal for this reaction.

3.3. Angular correlation parameters

By measuring the angular correlation between an electron which has excited the 2p level and the subsequently emitted photon, information can be obtained about the population of the magnetic substates. The measurements can be expressed in terms of the parameters R and λ defined by

$$\sigma R = \text{Re}\langle a_0 a_1 \rangle$$

$$\sigma \lambda = \sigma_0$$

where σ_0 and σ_1 are the cross sections for exciting the $2p_0$ and $2p_1$ levels ($\sigma = \sigma_0 + 2\sigma_1$) and a_0 and a_1 are the corresponding amplitudes.

In table 4 the calculated parameters R and λ are shown together with the calculated values of I , where

$$\sigma I = \text{Im}\langle a_0 a_1 \rangle.$$

Measurements, over the angular region from 10 to 140° at 54 eV, of R and λ by Williams (1981) have been included in table 4 and in figures 2 and 3. Also included are the results of the three-state close-coupling calculations of Burke *et al* (1980), which are not very different from our own. Other measurements of R and λ by

Table 4. Angular correlation parameters, $\lambda = \sigma_0/(\sigma_0 + 2\sigma_1)$ and $R = \text{Re}(a_0a_1)/\sigma$; also $I = \text{Im}(a_0a_1)/\sigma$.

$\theta(\text{deg})$	54 eV						100 eV						200 eV					
	Expt			A			C			A			A			A		
	R	λ		R	I	λ	R	λ		R	I	λ	R	I	λ	R	I	λ
0	—	—		0	0	1.0	0	1.0		0	0	1.0	0	0	1.0	0	0	1.0
10	0.28 (3)	0.34 (5)		0.33	-0.037	0.32	0.30	0.28		0.25	-0.036	0.15	0.17	-0.038	0.067	0.17	-0.038	0.067
20	0.21 (2)	0.23 (3)		0.27	-0.075	0.20	0.23	0.19		0.24	-0.096	0.16	0.23	-0.14	0.18	0.23	-0.14	0.18
30	0.18 (2)	0.55 (4)		0.26	-0.18	0.29	0.23	0.33		0.29	-0.19	0.45	0.31	0.058	0.66	0.31	0.058	0.66
40	0.122 (18)	0.82 (6)		0.22	-0.16	0.67	0.22	0.68		0.23	0.074	0.80	0.19	0.24	0.70	0.19	0.24	0.70
60	0.082 (3)	0.92 (6)		0.19	0.19	0.78	0.10	0.93		0.18	0.28	0.63	0.18	0.29	0.58	0.18	0.29	0.58
80	—	—		0.20	0.24	0.72	0.11	0.81		0.23	0.27	0.59	0.24	0.23	0.54	0.24	0.23	0.54
100	-0.113 (33)	0.35 (3)		0.20	0.21	0.76	0.16	0.81		0.26	0.22	0.63	0.25	0.15	0.65	0.25	0.15	0.65
120	-0.065 (3)	0.53 (4)		0.18	0.15	0.86	0.17	0.89		0.25	0.14	0.78	0.15	0.14	0.77	0.15	0.14	0.77
140	-0.056 (4)	0.90 (4)		0.12	0.084	0.95	0.12	0.96		0.20	0.090	0.88	0.09	0.015	0.76	0.09	0.015	0.76
160	—	—		0.055	0.023	0.99	—	—		0.11	0.051	0.97	0.002	0.092	0.68	0.002	0.092	0.68
180	—	—		0.0	0.0	1.0	0.0	1.0		0	0	1.0	0	0	1.0	0	0	1.0

Expt, Williams (1981); A, present results; C, three-state close-coupling (Burke *et al* 1980).

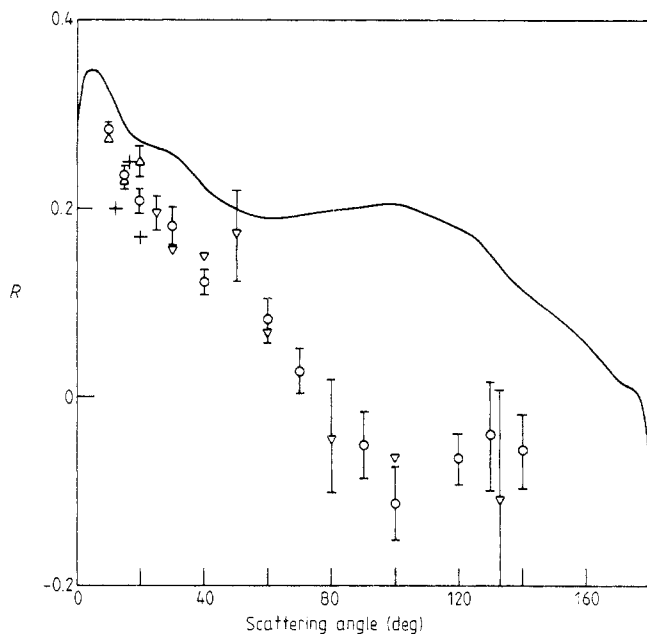


Figure 2. The parameter $R = \text{Re}(a_0 a_1) / \sigma$ at 54 eV. The full curve represents the results of the present calculation. The experimental data points are: \circ , Williams (1981); ∇ , Weigold *et al* (1980); +, Slevin *et al* (1980). Not all the experimental errors are shown for the sake of clarity.

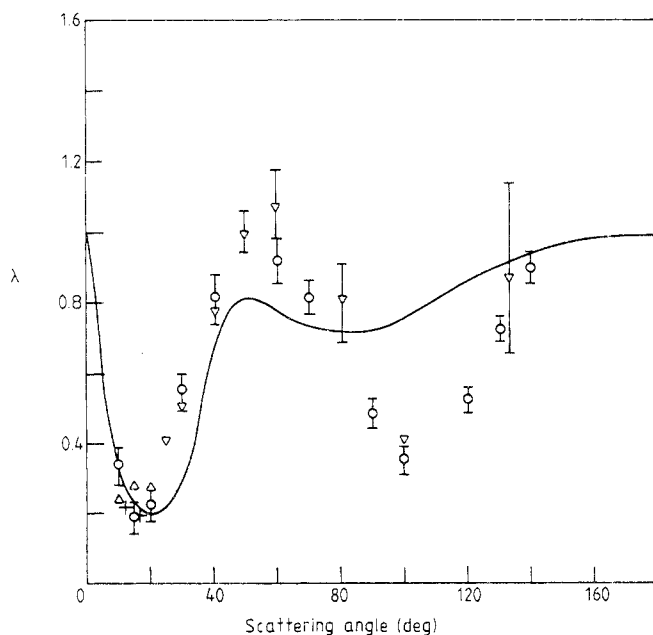


Figure 3. The parameter $\lambda = \sigma_0 / \sigma$. The notation is as in figure 2.

Weigold *et al* (1980) and Slevin *et al* (1980) at 54 eV agree reasonably with the data of Williams. Neither the present calculations nor the three-state close-coupling calculation agree with the data at all well. The disagreement is particularly marked for R , while in the case of λ although agreement is lacking at large angles, it is fair for $\theta < 80^\circ$.

At 100 eV measurements of R and λ (Slevin *et al* 1980, Hood *et al* 1979) are confined to small angles $\theta < 20^\circ$. These results are compared with our own in table 5. It would appear that there is little agreement at this energy between the theory and the data, although it would be desirable to have further measurements extending to larger angles.

Table 5. The angular correlation parameters at 100 eV.

θ (deg)	R			λ		
	E1	E2	P	E1	E2	P
3	0.23	—	—	0.39	—	—
5	0.19	—	0.32	0.09	—	0.30
10	0.15	0.175	0.25	0.02	0.194	0.14
15	0.11	0.148	0.23	0.18	0.183	0.13

E1, experimental measurements (Slevin *et al* 1980).

E2, experimental measurements (Hood *et al* 1979).

P, present results.

4. Conclusions

The present model appears to provide a satisfactory description of elastic scattering at 100 eV and above, but at 54 eV the results (and those of the R -matrix pseudostate close-coupling model) are less good than those of the single-channel optical potential models, and this can be attributed to the more restricted basis set employed. In the case of excitation, the calculated cross sections do not provide the marked improvement over those of the three-state close-coupling model that might have been expected. In particular, no model, including the present one, has been able to explain the behaviour of the R and λ parameters at 54 eV, or at 100 eV, and this again may point to the need for a larger basis set. In contrast, at small angles and at 100 and 200 eV, the results are close to those of the closure model, from which one would conclude that the basis set is adequate at 100 eV and above. For elastic scattering the third-order optical potential terms have been shown to be small by Byron and Joachain, but this is not necessarily the case for inelastic scattering and this remains a subject for future investigation.

Acknowledgments

Part of this work was supported by a grant from the Science and Engineering Research Council. One of us (BHB) would like to thank the Joint Institute for Laboratory Astrophysics for a Visiting Fellowship during part of the time this work was carried out.

References

- Bransden B H 1982 *Atomic Collision Theory* 2nd edn (New York: Benjamin)
- Bransden B H and Coleman J P 1972 *J. Phys. B: At. Mol. Phys.* **5** 537–45
- Bransden B H and McDowell M R C 1977 *Phys. Rep.* **30** 207–303
- Bransden B H and Noble C J 1976a *J. Phys. B: At. Mol. Phys.* **9** 1507–17
- 1976b *J. Phys. B: At. Mol. Phys.* **9** 2461–8
- 1976c *Aust. J. Phys.* **29** 165–9
- Burke P G, Fon W C, Kingston A E and Liew Y C 1980 (quoted by Williams 1981 as private communication)
- Byron F W and Joachain C J 1977 *J. Phys. B: At. Mol. Phys.* **10** 207–25
- 1981 *J. Phys. B: At. Mol. Phys.* **14** 2429–48
- Byron F W and Latour L J 1976 *Phys. Rev. A* **13** 649–64
- Callaway J, McDowell M R C and Morgan L A 1975 *J. Phys. B: At. Mol. Phys.* **8** 2180–90
- Ermolaev A M and Walters H R J 1979 *J. Phys. B: At. Mol. Phys.* **12** L779–84
- Fon W C, Berrington K A, Burke P G and Kingston A E 1981 *J. Phys. B: At. Mol. Phys.* **14** 1041–51
- de Heer F J, McDowell M R C and Wagenaar R W 1977 *J. Phys. B: At. Mol. Phys.* **10** 1945–53
- Hood S T, Weigold E and Dixon A J 1979 *J. Phys. B: At. Mol. Phys.* **12** 631–48
- Kauppila W E, Ott W R and Fite W L 1970 *Phys. Rev. A* **1** 1099–108
- Kingston A E, Fon W C and Burke P G 1976 *J. Phys. B: At. Mol. Phys.* **9** 605–18
- Long R L, Cox D M and Smith S J 1968 *J. Res. NBS A* **72** 521–35
- Martir M H, Ford A L, Reading J F and Becker R L 1982 *J. Phys. B: At. Mol. Phys.* **15** 1729–48
- McCarthy I E, Saha B C Stelbovics A T 1981 *Phys. Rev. A* **23** 145–52
- 1982 *J. Phys. B: At. Mol. Phys.* **15** L401–4
- Reid R H G, Kingston A E and Jamieson M J 1977 *J. Phys. B: At. Mol. Phys.* **10** 55–70
- Scott T and Bransden B H 1981 *J. Phys. B: At. Mol. Phys.* **14** 2277–2289
- Slevin J, Eminyan M, Woolsey J M, Vasselev G and Porter H O 1980 *J. Phys. B: At. Mol. Phys.* **13** L341–5
- Walters H R J 1980 *J. Phys. B: At. Mol. Phys.* **13** L749–55
- Weigold E, Frost L and Nygaard K J 1980 *Phys. Rev. A* **21** 1950–4
- Williams J F 1975 *J. Phys. B: At. Mol. Phys.* **8** 2191–9
- 1981 *J. Phys. B: At. Mol. Phys.* **14** 1197–217
- Williams J F and Willis B A 1975 *J. Phys. B: At. Mol. Phys.* **8** 1641–69
- Winters K H, Clark C D, Bransden B H and Coleman J P 1974 *J. Phys. B: At. Mol. Phys.* **7** 788–98